

Giant improvement of thermoelectric power factor of Bi_2Te_3 under pressure

Sergey V. Ovsyannikov,¹ Vladimir V. Shchennikov,^{1,a)} Grigoriy V. Vorontsov,¹
 Andrey Y. Manakov,² Anna Y. Likhacheva,³ and Vladimir A. Kulbachinskii⁴

¹High Pressure Group, Institute of Metal Physics, Urals Division, Russian Academy of Sciences, GSP-170,
 18 S. Kovalevskaya Str., Yekaterinburg 620041, Russia

²A.V. Nikolaev Institute of Inorganic Chemistry, Siberian Division, Russian Academy of Sciences,
 Novosibirsk 630090, Russia

³Institute of Mineralogy and Petrography, Siberian Division, Russian Academy of Sciences,
 Novosibirsk 630090, Russia

⁴Physics Department, M.V. Lomonosov Moscow State University, Moscow 119991, Russia

(Received 4 January 2008; accepted 22 June 2008; published online 9 September 2008)

The pressure (P) dependencies of both the thermopower (Seebeck effect) S and the electrical resistance (R) for p -type single crystals of Bi_2Te_3 and indium-doped bismuth telluride ($\text{In}_x\text{Bi}_{2-x}\text{Te}_3$, $0.04 \leq x \leq 0.10$) are reported on a pressure range of 0–8.5 GPa. The thermoelectric power factor (efficiency) ($\alpha = S^2/R$) exhibits two maxima: the first one near ~ 1 GPa and the second near ~ 2.5 – 4.5 GPa. These features evidence a giant increase in the power factor by a factor of ~ 10 . Possible values of the dimensionless figure of merit under pressure are also estimated. The maxima are explained in terms of pressure-driven changes in an electron structure. The second feature may be also addressed to an intermediate high-pressure phase detected in x-ray diffraction studies. © 2008 American Institute of Physics. [DOI: 10.1063/1.2973201]

I. INTRODUCTION

The principal task in the field of thermoelectric (TE) materials is the search for ways for the improvement of their TE parameters, namely, the power factor ($\rho = S^2/r$) and the dimensionless figure of merit [$ZT = TS^2/(\rho\lambda)$], where S is the thermopower, ρ is the electrical resistivity, λ is the thermal conductivity, and T is the temperature.^{1,2} Bismuth telluride (Bi_2Te_3) is one of the oldest among the basic materials for high-performance TE elements.¹ An exclusiveness of Bi_2Te_3 consists in the fact that the maximum of its figure of merit is achieved around room temperature.² Along with traditional n -type Bi_2Te_3 -based TE compounds, p -type Bi_2Te_3 and related structures are also promising for TE technologies, and in some cases exhibit higher TE parameters than those of the former.^{3–6} Nowadays, the TE parameters of Bi_2Te_3 are optimized by “technological factors” such as (i) doping and ion substitution [CsBi_4Te_6 ,⁵ $(\text{Bi}, \text{Sb})_2(\text{Te}, \text{Se}, \text{S})_3$],^{6–8} (ii) variation in mesostructure (nanostructures, superlattices, quantum dots, and wires),^{3,9–15} and (iii) variation in synthesis conditions.^{15–18} A permanent search for alternative room-temperature TE materials is under way.¹⁹ Effects of pressure and magnetic field on the TE properties of Bi_2Te_3 were investigated in only a few works.^{20,21}

At ambient conditions Bi_2Te_3 adopts a rhombohedral lattice of the $R\bar{3}m$ space group.²² The cell parameters of Bi_2Te_3 in terms of hexagonal axes are as follows: $a_H = 4.383$ Å and $c_H = 30.487$ Å.²² Pressure application was established to lead to the transitions first to an intermediate phase and then to a metal one, respectively, near ~ 6.7 and ~ 8.3 GPa at room temperature.²³ The intermediate phase was also detected by jumps in temperature dependencies of the electrical resistivity.²³ It was found that the intermediate phase has the

same space group ($R\bar{3}m$) but is characterized by a differing ratio from a_H to c_H (at elevated temperature: $a_H = 4.417$ Å and $c_H = 29.84$ Å).²³ Meanwhile, the structure of the metal phase remains obscure. At low temperatures all the three phases are superconducting and show different behaviors of the critical temperature $T_c(P)$.²⁴ A later study on pressure effect on the thermopower and the electrical resistivity of heavily doped samples (carrier concentrations: n , $p \sim 10^{19}$ cm⁻³) found only the transition to the metal above ~ 6.5 GPa for room temperature and suggested a weak influence of pressure on the power factor.²¹

In the present work we find stable anomalies in pressure dependencies of the thermopower of p -type $\text{In}_x\text{Bi}_{2-x}\text{Te}_3$ ($0 \leq x \leq 0.10$) (Fig. 1) resulting in the improvement in the TE power factor (efficiency) by a factor of ~ 10 – 40 (Fig. 2). In x-ray diffraction studies we find evidence for the intermediate high-pressure phase with a “distorted” rhombohedral lattice (Figs. 3 and 4).²²

II. EXPERIMENT

Two different anvil cells were employed for pressure generation: one of Bridgman-type made of synthetic diamonds with a working diameter of $d \sim 0.6$ mm and another one of toroidal shape made of tungsten-carbide hard alloy with a working diameter of the central semispherically concave anvils of $d \sim 1$ mm.^{25,26} In both cells a sample (of sizes of $\sim 200 \times 200 \times 30$ and $\sim 200 \times 200 \times 250$ μm^3 in the Bridgman and the toroidal cells, respectively) was put in a hole in a gasket made of the lithographic stone.^{25,26} The pressure values were determined with an uncertainty of $\sim 10\%$ from a calibration “stress-pressure” curve based on the known and well-detectable pressure-induced transitions in Bi, PbS, PbSe, CdSe, and in other compounds.²⁷ Applied force was measured by a digital dynamometer with resistive-

^{a)}Electronic mail: highpressgroup@mail.ru.

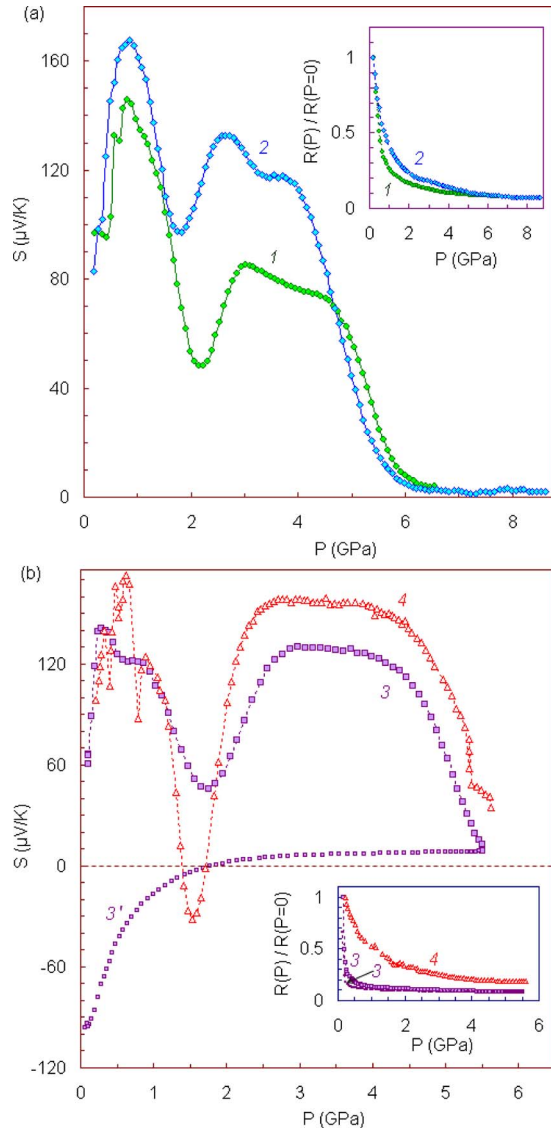


FIG. 1. (Color online) The pressure (P) dependencies of the TE power (S) of single crystals of $p\text{-Bi}_2\text{Te}_3$ (a) and $p\text{-In}_{0.04}\text{Bi}_{1.96}\text{Te}_3$ (b). The numbers mark the samples cut from the same ingot but measured in the different high-pressure cells with hard-alloy (1, 3) and diamond (2, 4) anvils. In the insets the corresponding pressure dependencies of the electrical resistance (R) are given in (b): 3': a decompression cycle for 3. Pressure treatment leads to an irreversible p - n inversion, and for the second pressure cycle a sample behaves like n -type material and exhibits a weak improvement in the power factor.

strain sensors.²⁸ The anvils were characterized by a high electrical conductivity, and therefore, were used as electrical outputs to a sample.²⁶ In the thermopower measurements an upper anvil was heated.²⁶ A temperature difference along a sample's thickness (ΔT) was determined from a temperature difference between the upper and the lower anvils; the latter was directly measured by means of the thermocouples. A calculation of a temperature distribution inside the anvils found that a potential divergence between the above temperature differences is within 20%.^{27,28} The pressure-independent uncertainty in ΔT gave the dominant contribution to the total error in determination of a value of the thermopower. To reduce this uncertainty in ΔT to $\sim 10\%$, several calibrated substances with the known ambient ther-

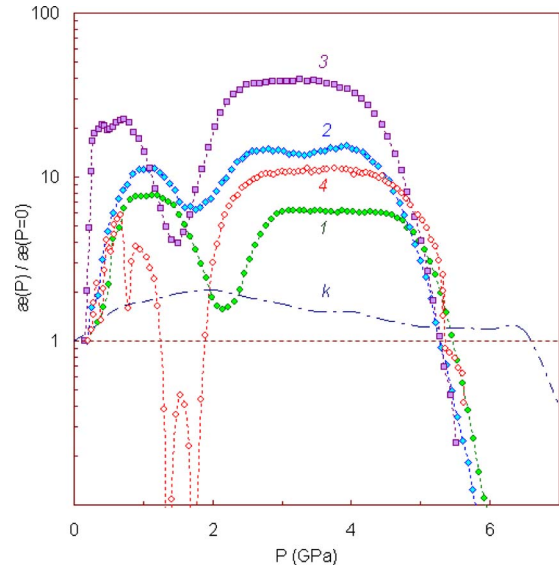


FIG. 2. (Color online) The pressure (P) dependencies of a relative change in the TE power factors (α) at $T=295$ K of $p\text{-Bi}_2\text{Te}_3$ and $p\text{-In}_{0.04}\text{Bi}_{1.96}\text{Te}_3$. The numbers correspond to Fig. 1. The dashed line k is a calculated dependence by the data from Ref. 21.

mopower values were measured, and after a comparison the corresponding correction factors were extracted. Possible small contribution to the thermopower from the anvils themselves was checked by measurement of lead ($S \approx -1.27 \mu\text{V/K}$).

The thermopower was measured in three regimes: at fixed temperature difference under gradual variation in pressure, at fixed pressure under variation in the temperature difference, and under variations both in P and in ΔT .^{25,26} All the

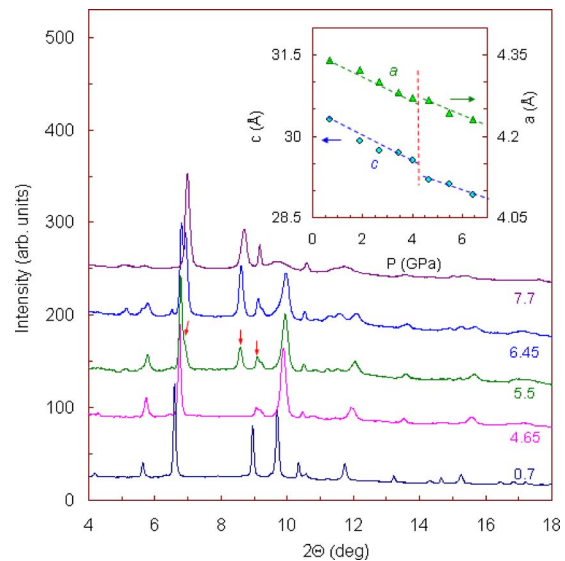


FIG. 3. (Color online) The x-ray diffraction patterns for $p\text{-In}_{0.10}\text{Bi}_{1.90}\text{Te}_3$ at $T=295$ K at selected pressures (given near the curves in gigapascal). At 5.5 GPa the reflexes from the metal high-pressure phase (marked by the arrows) appear. The reflexes originating from the rhombohedral structure persist at least up to 6.45 GPa. In the inset, the pressure (P) dependencies of the lattice parameters (a : right scale; c : left one) of the rhombohedral lattice are shown. A proposed border between the ambient rhombohedral lattice and the distorted one (the intermediate phase) is marked out by the dashed line. The error bars basically lie within the symbols.

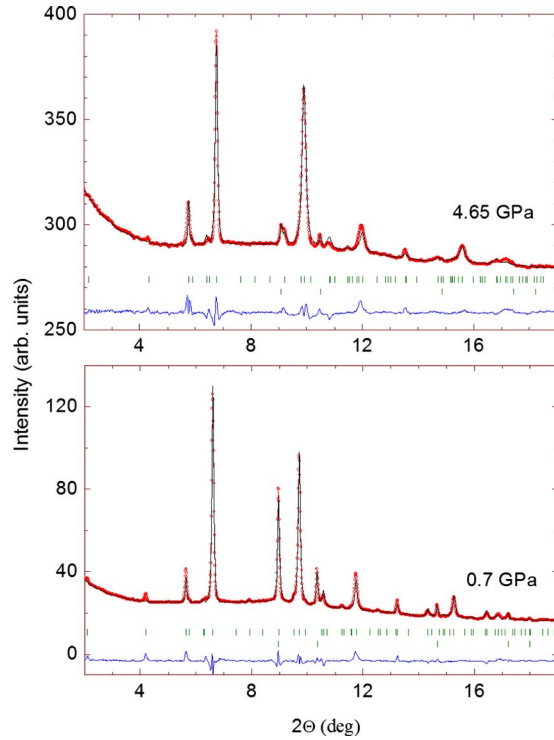


FIG. 4. (Color online) The examples of the Rietveld refinement of the x-ray diffraction patterns of *p*-type $\text{In}_{0.10}\text{Bi}_{1.90}\text{Te}_3$ at $T=295$ K (from Fig. 3). The lower pattern obtained at 0.7 GPa corresponds to the initial phase, and the upper one obtained at 4.65 GPa corresponds to the distorted phase. The points connected by the dashed lines are the experimental data. The solid lines are the calculated profiles for the rhombohedral structure (space group $R\bar{3}m$). The dashes below each curve show the reflectance position for the $R\bar{3}m$ space group (upper sets) and for Ag (lower sets). The lowermost curves in each plot show the difference between the experimental and the calculated profiles.

three methods gave the same results. The electrical resistance (R) was measured by a two-probe method with an uncertainty of $\sim 5\%$. The results gathered in both cells on thin and bulk samples were almost identical.

Structural properties under pressure were investigated in x-ray diffraction studies. The experiments were carried out on a station of the fourth channel of the VEPP-3 accelerator at the Budker Institute of Nuclear Physics of the Siberian Division of the Russian Academy of Sciences (Novosibirsk, Russia) in 0.3675 Å monochromatic synchrotron radiation. A MAR-3450 image plate detector was used to detect diffracted radiation. A diameter of the synchrotron beam was of ~ 5 μm. The experiments were performed at room temperature in a conventional diamond anvil cell with a methanol-ethanol pressure transmitting medium.²⁹ A sample was placed in a hole of ~ 0.2 mm diameter in a stainless-steel compressible gasket. The pressure values were determined by a change in the silver lattice parameter with an accuracy of ~ 0.1 GPa. The diffraction data were analyzed by means of the FULLPROF program for the profile analysis (Rietveld method),³⁰ and the unit cell parameters were refined using also the XLAT program.³¹

The single crystals of *p*-type $\text{In}_x\text{Bi}_{2-x}\text{Te}_3$ were grown by the Bridgman method and were characterized by the Hall concentrations for $x=0$ and 0.04, respectively, where $p=3 \times 10^{18}$ and 3×10^{17} cm⁻³ (at 4.2 K). At ambient conditions

TABLE I. The TE power factor [α in W/(K²m)] and the figure of merit (ZT) under pressure (P) (Figs. 1 and 2).

No. from Figs. 1 and 2	Sample	First maximum ($P \sim 0.5\text{--}1$ GPa)		Second maximum ($P \sim 2.5\text{--}3$ GPa)	
		$\alpha \times 10^3$	ZT	$\alpha \times 10^3$	ZT
1	Bi_2Te_3	4.44	0.81	3.68	0.57
2	Bi_2Te_3	4.81	0.87	6.61	1.02
3	$\text{In}_{0.04}\text{Bi}_{1.96}\text{Te}_3$	2.19	0.41	3.83	0.61
4	$\text{In}_{0.04}\text{Bi}_{1.96}\text{Te}_3$	1.76	0.33	3.39	0.54

the values of the resistivity and the thermal conductivity for $x=0(0.04)$ were found to be as follows: $\rho = 1.6(2.8)$ mΩ cm and $\lambda = 1.5(1.45)$ W/mK.^{32,33}

III. RESULTS

The pressure dependencies of the thermopower $S(P)$ of *p*- Bi_2Te_3 and *p*- $\text{In}_x\text{Bi}_{2-x}\text{Te}_3$ exhibit a nonmonotonic behavior (Fig. 1). Previously, in a pressure dependence of the thermopower of Bi_2Te_3 measured at liquid helium temperature, the strong oscillations were also registered.³⁴ These features were addressed to electronic topological transitions.³⁴ The increase in the thermopower with pressure to ~ 1 GPa and its drop above ~ 5 GPa are similar to those in previous studies.^{21,6} However, the abrupt drop in a value of the thermopower near $\sim 1.5\text{--}2$ GPa and the following wide maximum of that (Fig. 1) were not observed before.^{21,6} The curves of the electrical resistance against pressure (see the insets of Fig. 1) agree well with previous hydrostatic data reporting a decrease in the resistivity by approximately one order of magnitude to ~ 6 GPa.^{21,6} One can observe that some of the pressure dependencies of the electrical resistance also exhibit the weak anomalies near $\sim 2\text{--}4$ GPa (Fig. 1). The In substitution ($\text{In}_x\text{Bi}_{2-x}\text{Te}_3$ samples) shifts the drop in the $S(P)$ curves to the lower pressure values and enhances the second maximum in the thermopower [Fig. 1(b)]. Notice that a pressure treatment leads to an irreversible *p*-*n* inversion of the type of conductivity [Fig. 1(b) and Ref. 21].

The dependencies of a variation in the power factor under pressure $\alpha(P)$ were calculated by the data on the thermopower and the electrical resistance (Fig. 1). The $\alpha(P)$ curves of all the crystals measured exhibit two regions of enhancement (Fig. 2). The first maximum of the power factor near ~ 1 GPa was already registered in both Bi_2Te_3 and related solid solutions ($\text{Bi}_{0.5}\text{Sb}_{1.5}\text{Te}_3$ and BaBiTe_3).^{21,6} Whereas, the second maximum showing a more significant improvement in the power factor in a wider pressure range (Fig. 2) is a finding of the present work. Notice that our pressure effects on the power factor exceed those reported previously.²¹ The maximal absolute value of the power factor that we achieve under pressure equals $\alpha = 6.61 \times 10^{-3}$ W/(K²m) (Table I), which is a new record for Bi_2Te_3 .¹⁶

In the preliminary x-ray diffraction studies we detected both the intermediate and the metal high-pressure phases (Figs. 3 and 4). For instance, in the case of $\text{In}_x\text{Bi}_{2-x}\text{Te}_3$ ($x=0.10$) the structural transition to the metal lattice of a dif-

ferent symmetry is seen above ~ 5.5 GPa by the appearance of new reflexes (Fig. 3). This transition pressure corresponds well to the thermopower data (Fig. 1). However, no apparent changes in the x-ray diffraction patterns, which could point the existence of the intermediate phase, were found until the metallization (Fig. 3). Figure 4 shows the examples of a fitting of the full profiles of the x-ray diffraction patterns obtained at 0.7 and 4.65 GPa (Fig. 3) by the rhombohedral $R\bar{3}m$ space group.²² It is seen that both the experimental patterns are well described by this symmetry (Fig. 4). The lattice parameters of the rhombohedral unit cell were determined from the Rietveld refinement of the profiles (see the inset of Fig. 3). Meanwhile, an apparent discontinuity in the pressure dependencies of the lattice parameters is seen around 4 GPa (see the inset of Fig. 3). This feature may be addressed to the earlier proclaimed distorted rhombohedral lattice.^{22,23} The changes in the lattice parameters of the distorted phase, relatively the ambient one (i.e., the increase in a_H and the decrease in c_H) (see the inset of Fig. 3), qualitatively agree with previous data gathered at elevated temperatures.²² The latter suggests a jump in the ratio of a_H to c_H during the transition.²²

IV. DISCUSSION

At the present moment there is no complete understanding on how pressure changes the band structure of $(\text{Bi,Sb})_2\text{Te}_3$.^{35,36} A six-valley model has been proposed both for the valence and the conducting bands of Bi_2Te_3 .^{24,37,38} Furthermore, two additional electron and hole bands have been detected,³⁷ the former lies above the basic ones by $\Delta E_c \approx 0.30$ eV and the latter below those by $\Delta E_v \approx 0.20$ eV.³⁷ The effective masses of electrons (m_e^*) and holes (m_h^*) were found to be, respectively, $\sim 0.11m_0$ and $\sim 0.525m_0$ for the main bands; likewise, $1.5m_0$ and $2.5m_0$ for these additional ones.²⁴ When a carrier concentration is higher than $\sim 5 \times 10^{18}$ cm⁻³ the additional bands begin filling up.³⁷ According to recent calculations,³⁹ the highest valence band lies along the Z - U direction in the Brillouin zone and exceeds the second one in energy by $\Delta E_v = 3.8$ meV (versus $\Delta E_v = 40$ meV of Ref. 40). While the two lowest conduction bands, located along the Γ - Z direction, differ by ~ 53 meV.³⁹

The indirect forbidden gap $E_g = 0.17$ eV of Bi_2Te_3 decreases with pressure with a kink around ~ 3 GPa ($dE_g/dP \approx -20$ and ≈ -60 meV/GPa, respectively, before and after that) and reaches zero near $P \sim 4.5$ – 5 GPa.^{24,37} At liquid helium temperature a pressure-driven upward shift of the “light” hole band relative to the “heavy” hole band has been estimated to have a rate $dE_v/dP \sim +30$ meV/GPa,³³ i.e., the energy gap between the hole bands (ΔE_v) increases with pressure contrary to the forbidden gap.

From the general expressions for the electrical conductivity (σ), $S: \sigma = -\int \sigma(E) (df/dE) dE$ and $S = -k/|e| \int [(E - E_F)/(kT)] [\sigma(E)/\sigma] (df/dE) dE$ (where f is the distribution function, E_F and E are, respectively, the Fermi and the electron energies, k is Boltzmann’s constant, and e is the electron charge), one can derive a formula for the Seebeck coefficient of a semiconductor with one additional hole band as follows:

$$\frac{S}{k/|e|} = \left\{ \sum_i \frac{(\sigma_{pi} - \sigma_{ni})}{\sigma} \times (r+2) + \sum_i \frac{(\sigma_{pi} - \sigma_{ni})}{\sigma} \frac{E_g}{2kT} + \frac{3}{4} \ln \frac{m_p^*}{m_n^*} + \frac{\Delta E_v}{kT} \frac{\sigma_{p2}}{\sigma} \right\}, \quad (1)$$

where $\sigma = \Sigma(\sigma_{ni} + \sigma_{pi})$ is the total conductivity and r is the scattering parameter of carriers. The index i corresponds to the electron and the hole bands and the index “2” to the additional hole band. Since pressure application leads to narrowing of the forbidden gap, and therefore, to the increase in the carrier concentration, it eventually brings to the intrinsic conductivity.

The first maximum in the thermopower registered near ~ 1 GPa (Fig. 1) could arise from a competition between the contributions of the basic hole and the electron bands under narrowing in the forbidden gap on the one hand, and a contribution of the additional hole band which is rising owing to the widening of ΔE_v [Eq. (1)]. Then, the contribution of the second hole band (σ_{p2}/σ) decreases, which leads to a diminishing in the thermopower (Fig. 1). For samples with low hole concentration ($p \leq 3 \times 10^{18}$ cm⁻³), the increase in the electron contribution to conductivity can even result in a sign inversion of the thermopower [Fig. 1(b)]. The second wide maximum of the thermopower found near ~ 2.5 – 4.5 GPa (Figs. 1 and 2) could originate from the distorted rhombohedral phase (Figs. 3 and 4).²² The improvement in the TE properties at the distorted phase (Figs. 1 and 2) correlates with a previously revealed enhancement of the superconductivity (T_c) in this phase.²⁴ The variation in the dE_g/dP coefficient found near 3 GPa (Refs. 24 and 37) hints at a change in the band extrema, which may be responsible for this growth in the thermopower (Fig. 1).

It seems interesting to estimate a possible pressure effect on the dimensionless figure of merit of the Bi_2Te_3 samples. The main obstacle in the estimation is the absence of data on pressure behavior of the thermal conductivity. Notice that only a few laboratories all over the world have facilities for such kind of measurements. As a consequence, *in situ* determination of a value of the figure of merit under high pressure was not hitherto reported. Even at ambient pressure, a direct measurement of the thermal conductivity in thin films seems to be hard and it is often substituted by different calculations.³ For example, the electronic part of the thermal conductivity (λ_e) is calculated by the Weidemann–Franz law as follows: $\lambda_e = L_0 T \sigma$, where L_0 is the Lorenz number.^{3,4} However, from the comparison of experimental data on pressure behavior of the thermal conductivity and of the electrical resistivity, those are available, for instance, for a kindred TE material adopting the same crystal structure Sb_2Te_3 ,^{41,42} it follows that the L_0 number greatly diminishes with pressure. It was also found that the lattice part of the thermal conductivity of Sb_2Te_3 is a very weak function of pressure at least up to 1.6 GPa.⁴¹ Therefore, in the case of Bi_2Te_3 one cannot surely calculate a pressure-induced variation in λ_e , under the assumption of the pressure-independent Lorenz number.

For Sb_2Te_3 it was reported that the total thermal conductivity grows with pressure by 13% to 1.6 GPa,⁴¹ and the

electrical resistivity decreases by approximately two orders of magnitude to $\sim 5\text{--}6$ GPa.⁴² Then, the values of the figure of merit, which are achieved in the Bi_2Te_3 samples under pressure, may be roughly estimated if we use the data on a pressure effect on the thermal conductivity for Sb_2Te_3 .⁴¹ Since the major influence of pressure on the thermal conductivity is related to the electronic part,⁴¹ and in the case of Sb_2Te_3 the pressure-induced decrease in the resistivity is more significant than the one in Bi_2Te_3 (two orders⁴² versus one order²¹), the above approach does not lead to an overestimation. Thus, in an estimation of the figure of merit of $\text{In}_x\text{Bi}_{2-x}\text{Te}_3$ we assumed a pressure-induced growth in the thermal conductivity by a factor of 1.1 and 1.3, respectively, for the first and the second maxima of the power factor (Fig. 2). The first factor (1.1) corresponded to the case of Sb_2Te_3 ,⁴¹ while the second one (1.3) was obtained by an extrapolation to higher pressures. Pressure dependencies of a temperature difference along a sample ΔT ($\Delta T = qh/\lambda$, where q is a density of a thermal flow and h is a sample's thickness)^{27,28} qualitatively evidence that a possible growth in the thermal conductivity to ~ 5 GPa is less than twofold. Then, the maximally accessible value of the figure of merit for our samples $ZT=1.02$ (Table I). This value is close to those in the "state-of-the-art" bulk $(\text{Bi},\text{Sb})_2\text{Te}_3$ thermoelectrics.¹⁻³

V. CONCLUSION

In summary, pressure application was established to lead to a significant improvement in the TE efficiency of $p\text{-Bi}_2\text{Te}_3$ by a factor of $\sim 10\text{--}40$. This effect excels that reported previously.²¹ The maximal power factor found in Bi_2Te_3 , $\alpha = 6.61 \times 10^{-3}$ W/(K² m), exceeds a previous record by $\sim 20\%$.¹⁶ As the maxima in the curves of TE power factor lie at low pressure values, a *HP-HT* synthesis of Bi_2Te_3 can result in a colossal improvement in both the power factor and the figure of merit.

ACKNOWLEDGMENTS

This work was supported by the RFBR (Grand No. 07-08-00338) and Siberian Division of RAS (Grant No. 43).

¹F. J. DiSalvo, *Science* **285**, 703 (1999).

²T. M. Tritt, *Science* **283**, 804 (1999).

³R. Venkatasubramanian, E. Siivola, T. Colpitts, and B. O'Quinn, *Nature (London)* **413**, 597 (2001).

⁴X. F. Tang, W. J. Xie, H. Li, W. Y. Zhao, Q. J. Zhang, and M. Niino, *Appl. Phys. Lett.* **90**, 012102 (2007).

⁵D.-Y. Chung, T. Hogan, P. Brazis, M. Rocci-Lane, C. Kannewurf, M. Bastea, C. Uher, and M. G. Kanatzidis, *Science* **287**, 1024 (2000).

⁶D. A. Polvani, J. F. Meng, N. V. Chandra Shekar, J. Sharp, and J. V. Badding, *Chem. Mater.* **13**, 2068 (2001), and references within.

⁷G. F. Wang and T. Cagin, *Appl. Phys. Lett.* **89**, 152101 (2006).

⁸V. A. Kutasov, L. N. Luk'yanova, and P. P. Konstantinov, *Phys. Solid*

State **42**, 2039 (2000).

⁹M. P. Singh and C. M. Bhandari, *Solid State Commun.* **127**, 649 (2003).

¹⁰X. B. Zhao, X. H. Ji, Y. H. Zhang, T. J. Zhu, J. P. Tu, and X. B. Zhang, *Appl. Phys. Lett.* **86**, 062111 (2005).

¹¹J. H. Zhou, C. G. Jin, J. H. Seol, X. G. Li, and L. Shi, *Appl. Phys. Lett.* **87**, 133109 (2005).

¹²S. Lee and P. von Allmen, *Appl. Phys. Lett.* **88**, 022107 (2006).

¹³G. E. Bulman, E. Siivola, B. Shen, and R. Venkatasubramanian, *Appl. Phys. Lett.* **89**, 122117 (2006).

¹⁴B. Yang and Z. H. Han, *Appl. Phys. Lett.* **89**, 083111 (2006).

¹⁵H. L. Ni, X. B. Zhao, T. J. Zhu, X. H. Ji, and J. P. Tu, *J. Alloys Compd.* **397**, 317 (2005).

¹⁶O. Yamashita, S. Tomiyoshi, and K. Makita, *J. Appl. Phys.* **93**, 368 (2003).

¹⁷J. Walachova, R. Zeipl, J. Zelinka, V. Malina, M. Pavelka, M. Jelinek, V. Studnicka, and P. Lost'ak, *Appl. Phys. Lett.* **87**, 081902 (2005).

¹⁸T. C. Su, P. W. Zhu, H. A. Ma, G. Z. Ren, L. X. Chen, W. L. Guo, Y. Iami, and X. P. Jia, *Solid State Commun.* **138**, 580 (2006).

¹⁹N. D. Lowhorn, T. M. Tritt, E. E. Abbott, and J. W. Kolis, *Appl. Phys. Lett.* **88**, 022101 (2006).

²⁰A. A. Averkin, O. S. Gryaznov, and Y. Z. Sanfirov, *Sov. Phys. Semicond.* **12**, 1358 (1978).

²¹L. G. Khvostantsev, A. I. Orlov, N. K. Abrikosov, T. E. Svechnikova, and S. N. Chizhevskaya, *Phys. Status Solidi A* **71**, 49 (1982).

²²E. Y. Atabaeva, E. S. Itskevich, S. A. Mashkov, S. P. Popova, and L. F. Vereshchagin, *Sov. Phys. Solid State* **10**, 43 (1968).

²³L. F. Vereshchagin, N. A. Bendeliani, and E. Y. Atabaeva, *Sov. Phys. Solid State* **13**, 2051 (1972).

²⁴M. A. Ilina and E. S. Itskevich, *Fiz. Tverd. Tela (Leningrad)* **17**, 154 (1975).

²⁵S. V. Ovsyannikov and V. V. Shchennikov, *J. Phys.: Condens. Matter* **18**, L551 (2006).

²⁶S. V. Ovsyannikov and V. V. Shchennikov, *Appl. Phys. Lett.* **90**, 122103 (2007).

²⁷V. V. Shchennikov, S. V. Ovsyannikov, and A. V. Bazhenov, "A composite high-pressure cell with sintered diamond insets for study of thermoelectric and thermomagnetic properties in a range up to 30 GPa: Application to Pr and PbTe." *J. Phys. Chem. Solids* (to be published).

²⁸V. V. Shchennikov, S. V. Ovsyannikov, A. Y. Derevskov, and V. V. Shchennikov, Jr., *J. Phys. Chem. Solids* **67**, 2203 (2006).

²⁹V. V. Shchennikov, S. V. Ovsyannikov, A. Y. Manakov, A. Y. Likhacheva, A. I. Ancharov, I. F. Berger, and M. A. Sheromov, *JETP Lett.* **83**, 228 (2006).

³⁰J. Rodriguez-Carvajal, *Physica B & C* **192**, 55 (1993).

³¹B. Rupp, *Scr. Metall.* **22**, 1 (1988).

³²A. E. Kar'kin, V. V. Shchennikov, B. N. Goshchitskii, S. E. Danilov, V. L. Arbuзов, and V. A. Kul'bachinskii, *Phys. Solid State* **45**, 2249 (2003).

³³V. A. Kulbachinskii, N. E. Klokov, J. Gorak, P. Lostjak, S. A. Azou, and G. A. Mironova, *Fiz. Tverd. Tela (Leningrad)* **31**, 205 (1989).

³⁴E. S. Itskevich, L. M. Kashirskaya, and V. F. Kraidenov, *Semiconductors* **31**, 276 (1997).

³⁵P. Larson, *Phys. Rev. B* **74**, 205113 (2006).

³⁶S. K. Mishra, S. Satpathy, and O. Jepsen, *J. Phys.: Condens. Matter* **9**, 461 (1997).

³⁷B. M. Goltzman, B. A. Kudinov, and I. A. Smirnov, *Thermoelectric Semiconductor Materials Based on Bi₂Te₃* (Nauka, Moscow, 1972).

³⁸V. A. Greanya, W. C. Tonjes, R. Liu, C. G. Olson, D. Y. Chung, and M. G. Kanatzidis, *Phys. Rev. B* **62**, 16425 (2000).

³⁹S. J. Youn and A. J. Freeman, *Phys. Rev. B* **63**, 085112 (2001).

⁴⁰T. J. Scheidmantel, C. Ambrosch-Draxl, T. Thonhauser, J. V. Badding, and J. O. Sofo, *Phys. Rev. B* **68**, 125210 (2003).

⁴¹A. A. Averkin, Z. Z. Zhaparov, and L. S. Stilbans, *Sov. Phys. Semicond.* **5**, 1954 (1972).

⁴²N. Sakai, T. Kajiwara, K. Takemura, S. Minomura, and Y. Fujii, *Solid State Commun.* **40**, 1045 (1981).